Analytical Approach to the Recovery of Short Fluorescence Lifetimes from Fluorescence Decay Curves

Željko Bajzer*, Antonio Zelić,*§ and Franklyn G. Prendergast‡
*Department of Biochemistry and Molecular Biology, Mathematical Methods Core Facility, ‡Department of Pharmacology, Mayo Foundation, Rochester, Minnesota 55905; and §Division of Applied Mathematics, Brown University, Providence, Rhode Island 02912 USA

ABSTRACT Considerable effort in instrument development has made possible detection of picosecond fluorescence lifetimes by time-correlated single-photon counting. In particular, efforts have been made to narrow markedly the instrument response function (IRF). Less attention has been paid to analytical methods, especially to problem of discretization of the convolution integral, on which the detection and quantification of short lifetimes critically depends. We show that better discretization methods can yield acceptable results for short lifetimes even with an IRF several times wider than necessary for the standard discretization based on linear approximation (LA). A general approach to discretization, also suitable for nonexponential models, is developed. The zero-time shift is explicitly included. Using simulations, we compared LA, quadratic, and cubic approximations. The latter two proved much better for detection of short lifetimes and, in that respect, they do not differ except when the zero-time shift exceeds two channels, when one can benefit from using the cubic approximation. We showed that for LA in some cases narrowing the IRF beyond *FWHM* = 150 ps is actually counterproductive. This is not so for quadratic and cubic approximations, which we recommend for general use.

INTRODUCTION

There is currently substantial interest in the detection and quantification of picosecond events in biological systems. With the advent and now rapidly expanding use of molecular dynamics simulations, the need to measure the rate and amplitude of motions presumably occurring on a picosecond time scale has grown more marked. On the one hand, the need is simply to ascertain whether such dynamics events *can* actually be reliably determined but, on the other hand, it is important to be able to quantify reliably picosecond mobility if we are to validate inferences drawn from simulations. Two techniques dominate the experimental studies of picosecond dynamics, NMR-relaxation methodologies and time-resolved fluorescence decay measurements. In this paper, we are concerned about the latter.

The usefulness of time-resolved fluorescence techniques for the study of macromolecular structure and dynamics depends on the confidence we have in the recovered decay parameters, which in turn depend on the accuracy and sensitivity of the methods used for data analysis. For the time-correlated single-photon counting, many of the analytical methods (such as least-squares (Grivald and Steinberg, 1974), maximum likelihood (Bajzer et al., 1991), exponential series (Ware et al., 1973), and maximum entropy (Livesey and Brochon, 1987)) rely critically on the reliability of iterative deconvolution, which in turn requires suitable discretization of the convolution integrals involved. This issue becomes especially important when detection of the very short fluorescence lifetimes or fluorescence anisotropy decays are considered. Interestingly, much of the effort toward the determination of picosecond fluorescence events has focused on instrumentation. Particular attention has been paid to ways to minimize the width of the instrument response function (IRF) through use of very fast microchannel plate photomultiplier tubes and state-of-the-art electronic components. Much less attention has been paid to numerical procedures used in the discretization of convolution integrals and yet, as we will demonstrate here, better discretization methods can afford acceptable results for short lifetimes even with an IRF several times wider than those currently considered necessary for the discretization methods now used most frequently.

Until recently, two discretization schemes have been used generally: the GS technique (Grinvald and Steinberg, 1974) based on the first mean value theorem for integrals and the piecewise linear approximation of IRF (cf. Bajzer and Prendergast, 1992), and the scheme based on linear approximation (LA) of the IRF proposed by McKinnon et al. (1977) and later independently derived in more detail by Wahl (1979). Periasamy (1988) has performed extensive simulations comparing these two discretization schemes and showed that the LA scheme is definitely preferable to the GS scheme. There was also an unexpected result in that fluorescence lifetimes equal to or shorter than the channel width could be detected with fair accuracy. More recently, we have proposed another scheme (Bajzer et al., 1991) based on the generalized first mean value theorem for integrals (GMTV) and compared it with the other two methods by use of simulations. That comparison was not very extensive and basically confirmed the results of Periasamy. The GMVT scheme was ranked somewhere between the other two; in fact, the GMVT scheme emerged in

Received for publication 17 January 1995 and in final form 17 May 1995.
Address reprint requests to Dr. Željko Bajzer, Rm. 1042 B Guggenheim, Mayo Clinic and Foundation, 200 First Street SW, Rochester, MN 55905. Tel.: 507-284-8584; Fax: 507-284-9420; E-mail: bajzer@mayo.edu.

0006-3495/95/09/1148/14 $2.00

simulations for two-exponential models as a good compromise for a wide range of lifetime ratios.

In discussing the options for measurements of fast fluorescence events, Holtom (1990) has proposed a scheme founded on quadratic approximation (QA). However, he neither presented any details of its derivation nor provided a comparative study that would demonstrate the relative merit of such a discretization scheme. Most recently, in an excellent paper Večeř et al. (1993) derived a discretization scheme for a polynomial interpolation of any order. Their formula is a direct generalization of Wahl's formula (Wahl, 1979) and, therefore, is valid for multiexponential decay only. To our best knowledge, the discretization for nonexponential models so far has been restricted only to piecewise constant approximation (see, e.g., Argyrakis et al., 1991). The approach we describe conveniently allows higher order polynomial approximations to be made for nonexponential and multiexponential models. The mathematical basis is Fubini's theorem. Its particular application to involved integrals leads to a form in which a given approximation of the IRF can be used within a single-channel width, whereas in the approach of Wahl (1979) and Večeř et al. (1993), a given approximation of the IRF was used within two channels. In addition to that, we explicitly included a nontrivial correction for the zero-time shift—a feature that we have not found in any published papers.

Besides deriving general discretization formulae, we investigate the relative merit of linear, quadratic, and cubic approximation for the multiexponential model by numerous simulations of heterogeneous fluorescence intensity decays. Each of these includes one very short lifetime. One set of simulated data was based on actually measured three-component decay found in study of tryptophan fluorescence in human recombinant interferon α_2 (Vincent et al., 1992). Our aim is to find which polynomial approximation yields reliable estimation of the shortest possible lifetime. Special attention is paid to evaluation of linear, quadratic, and cubic approximations under various conditions with respect to width of the IRF, zero-time shift, light scattering correction, signal-to-noise ratio, and channel width. In this respect, our work complements the work of Večeř et al. (1993). They evaluated the effectiveness of polynomial approximations—up to the fourth order—on carefully chosen simulated data, but did not discuss the effects of the width of the IRF or the zero-time shift. Our results generally agree with their principal conclusions, namely, that higher order polynomial approximations are advantageous in the analysis of TCSPC data.

DERIVATION OF DISCRETIZATION FORMULAE

Basic equations

In a typical time-correlated single-photon counting experiment, the counts f_i in channel i associated with known fluorescence intensity decay function $I(t) \leq 0$ are modeled as (see O'Connor and Phillips, 1978):

$$f_i = F_i + \xi R_i + b, \qquad F_i = \int_{t_{i-1}}^{t_i} dt \int_0^t R(u+\delta) I(t-u) du, \tag{1}$$

where $R(t)$ is the instrument response function (or excitation function) represented by counts in channel i:

$$R_i = \int_{t_{i-1}}^{t_i} R(t) dt, \qquad R(t) \geq 0, \qquad i = 1, \ldots, n \tag{2}$$

$\xi \geq 0$ represents a parameter determining the light scattering correction and b is the preassumed constant background. The parameter δ is the zero-time shift and

$$t_i = ih, \qquad i = 0, 1, \ldots, n, \qquad h > 0, \tag{3}$$

where h denotes channel width (time calibration). For mathematical purposes, the functions $R(t)$ and $I(t)$ are assumed to have continuous first derivatives in the interval $(0, nh]$ and $R(t) \equiv 0$, $t \leq 0$, $I(t) \equiv 0$, $t < 0$. It is important to stress that $R(t)$ is an unknown function, whereas $I(t)$ is either known analytically or can be evaluated numerically to arbitrary precision.

As Večeř et al. (1993) have pointed out recently, the function $R(t)$ is not experimentally attainable (which has often been assumed) but, rather, the number of counts R_i is measurable. Therefore, we introduce the integrated IRF (designated as "count function") $\rho_i(t)$, which is naturally related to R_i, namely, $\rho_i(t_i) = R_i$. This function is generally defined by

$$\rho_i(t) = \int_{t_{i-1}}^{t} R(u) du, \quad i \geq 1, \quad \rho_0(t) \equiv 0. \tag{4}$$

and has the following useful properties based on its definition, on Eq. 2, and $R(t) \equiv 0$, $t \leq 0$:

$$\partial \rho_i(t)/\partial t = R(t), \tag{5}$$

$$\rho_i(t) = -\sum_{\nu=1}^{i-1} R_\nu = -S_i, \quad i = 2, \ldots, n, \quad \rho_1(t) \equiv 0, \quad t \leq 0, \tag{6}$$

$$\rho_i(t_{i+k}) = \sum_{\nu=0}^{k} R_{i+\nu}, \tag{7}$$

$$i = 1, \ldots, n, \quad k = 0, 1, \ldots, n-i,$$

$$\rho_i(t_{i-1}) = 0, \quad i = 1, \ldots, n, \tag{8}$$

$$\rho_i(t_{i-k}) = -\sum_{\nu=1}^{k-1} R_{i-k+\nu}, \quad i = 2, \ldots, n, \quad k = 2, \ldots, i. \tag{9}$$

When the zero-time shift is different from zero, it is also

convenient to define the function

$$\rho_i(t,\delta) = \rho_i(t+\delta) - \rho_i(t_{i-1}+\delta) = \int_{t_{i-1}}^{t} R(u+\delta)du. \quad (10)$$

Discretization

In the following, we consider discretization of integrals in Eq. 1 that we wish to express in terms of known quantities R_i and $I(t)$. First, F_i can be rewritten as

$$F_i = \int_{t_{i-1}}^{t_i} dt \int_0^{t_{i-1}} R(u+\delta)I(t-u)du + \int_{t_{i-1}}^{t_i} dt \int_{t_{i-1}}^{t} R(u+\delta)I(t-u)du, \quad (11)$$

The first term in this equation can be expressed as $\sum_{j=1}^{i-1} \int_{t_{i-1}}^{t_i} dt \int_{t_{j-1}}^{t_j} R(u+\delta)I(t-u)du$, and in the second term the integrations can be interchanged to yield

$$\int_{t_{i-1}}^{t_i} dt \int_{t_{i-1}}^{t} R(u+\delta)I(t-u)du = \int_{t_{i-1}}^{t_i} du \int_{u}^{t_i} R(u+\delta)I(t-u)dt. \quad (12)$$

This is based on Fubini's theorem (see, e.g., Rade and Westergren, 1990), which states that for an integrable function $f(t,u) \geq 0$ double integration is interchangeable: $\int_a^b dt \int_c^d f(t,u)du = \int_c^d du \int_a^b f(t,u)dt$. Now, if we specify $a = c = t_{i-1}$; $b = d = t_i$ and $f(t,u) = R(u+\delta)I(t-u)$ for $t_{i-1} \leq u \leq t \leq t_i$, whereas $f(t,u) = 0$ for $t_{i-1} < t < t_i$, $u > t$, then Eq. 12 follows in a straightforward manner. Thus, Eq. 11 can be rewritten as

$$F_i = B_i + \sum_{j=1}^{i-1} B_{ij}, \quad i = 2,\ldots,n, \quad F_1 = B_1,$$

$$B_{ij} = \int_{t_{j-1}}^{t_j} R(u+\delta)G_i(t_{i-1},u)du, \quad G_i(t,u) = \int_t^{t_i} I(v-u)dv, \quad (13)$$

$$B_i = \int_{t_{i-1}}^{t_i} R(u+\delta)G_i(u,u)du.$$

This formula for F_i represents a crucial step by which we have conveniently reduced the discretization problem to discretization of two similar one-dimensional integrals over a single channel. Both integrals involve the product of the unknown function $R(t)$ and the function $G_i(t,u)$, which can be evaluated numerically to arbitrary precision.

Before proceeding any further, we wish to compare this formula with the one obtained by Wahl (1979) for the exponential decay, $I(t) = e^{-t/\tau}$:

$$F_i - F_{i-1}e^{-h/\tau} = \int_{t_{i-1}}^{t_i} dt e^{-t/\tau} \int_{t-h}^{t} R(u)e^{u/\tau}du \quad (14)$$

To perform this double integration, the function $R(u)$ should be approximated within the interval $[t_{i-2}, t_i]$ comprising two channels. Wahl (1979), and subsequently Večeř et al. (1993), used the same approximation polynomial throughout these two channels. In our discretization scheme, Eq. 13 yields

$$F_i - F_{i-1}e^{-h/\tau} = B_i - B_{i-1}e^{-h/\tau} + B_{ii-1},$$

$$B_i = \tau(R_i - e^{-t_i/\tau}I_i), \quad B_{ij} = \tau e^{-t_i/\tau}(e^{h/\tau} - 1)I_j,$$

$$I_i = \int_{t_{i-1}}^{t_i} R(t)e^{t/\tau}dt.$$

Obviously, here $R(t)$ has to be known in the interval $[t_{i-1}, t_i]$, corresponding to one channel only. Consequently, unlike Wahl, we can naturally approximate $R(t)$ in each channel separately. In principle, Wahl or Večeř et al. could have also used the separate approximation for each channel, but this was not done, and in such a circumstance our formula offers a better starting point for approximation.

We could now proceed by approximating $R(t+\delta)$ to obtain F_i in terms of R_i. However, it is more convenient first to rewrite Eq. 13 in terms of a "count function" $\rho_i(t)$ and then subsequently introduce approximations of $\rho_i(t)$. Following this idea, we express the integral B_{ij} in terms of $\rho_j(x,\delta)$ by using partial integration, the properties of $G_i(x,y)$, and Eqs. 5 and 10:

$$B_{ij} = \int_{t_{j-1}}^{t_j} [\partial\rho_j(u,\delta)/\partial u]G_i(t_{i-1},u)du = A_{ij} + C_{ij} - C_{i-1j}, \quad (15)$$

where

$$A_{ij} = \rho_j(t_j,\delta) \int_{t_{i-1}}^{t_i} I(t-t_j)dt, \quad (16)$$

$$C_{ij} = \int_{t_{j-1}}^{t_j} \rho_j(t,\delta)I(t_i-t)dt. \quad (17)$$

In a similar way, $B_i = C_{ii}$ and Eq. 13 becomes

$$F_i = C_{ii} + \sum_{j=1}^{i-1} (A_{ij} + C_{ij} - C_{i-1j}), \quad i = 2,\ldots,n, \quad F_1 = C_{11}. \quad (18)$$

This is a general formula for discretization that can be applied to *any decay function* $I(t)$ and for *any type of approximation* for $\rho_j(t)$ (note that $\rho_j(t, \delta)$ in Eqs. 16 and 17 can be expressed by $\rho_j(t)$ via Eq. 10). When the multiexponential decay model

$$I(t) = \sum_{k=1}^{N} A_k e^{-t/\tau_k}, \quad A_k \geq 0, \quad \tau_k > 0. \tag{19}$$

is used, one can obtain F_i in a computationally convenient iterative form:

$$F_i = \sum_{k=1}^{N} F_i^k, \quad F_0 = F_0^k = 0, \tag{20}$$

$$F_i^k = D_k F_{i-1}^k + A_k \tau_k (1 - D_k)[\rho_{i-1}(t_{i-1} + \delta) - \rho_i(t_{i-1} + \delta)] + A_k D_k (J_i^k - J_{i-1}^k) \tag{21}$$

$$J_i^k = \int_0^h \rho_i(t + t_{i-1} + \delta) e^{t/\tau_k} dt, \quad i = 1, \ldots, n, \qquad J_0^k = 0, \quad D_k = e^{-h/\tau_k}. \tag{22}$$

This is now the most general discretization formula for multiexponential decay analysis. Depending on how we approximate the unknown function ρ_j, one can obtain different expressions for F_i that can be used directly for computational implementation.

Polynomial approximation

The function $\rho_j(t)$ for a given j can be approximated locally by a polynomial of some order m:

$$\rho_j(t) \approx \rho_j^m(t) = -\bar{\theta}(t) S_j + \theta(t) \sum_{\lambda=1}^{m} a_{j\lambda} (t - t_{j-1})^\lambda. \tag{23}$$

$$\theta(x) = 0, x \leq 0; \qquad \theta(x) = 1, x > 0; \qquad \bar{\theta}(x) = 1 - \theta(x) \tag{24}$$

Such approximation automatically satisfies Eqs. 6 and 8. The integral C_{ij} is then approximated by

$$C_{ij} \approx \theta(\delta) \sum_{\lambda=1}^{m} a_{j\lambda} \int_0^h [(x + \delta)^\lambda - \delta^\lambda] I(t_i - t_{j-1} - x) dx + \bar{\theta}(\delta) K_{ij}(\delta) \tag{25}$$

where $K_{ij}(\delta)$ is a quite complex expression given explicitly in the Appendix. According to Eq. 24, the second term of the above expression vanishes for $\delta > 0$ and the first term vanishes for $\delta \leq 0$. For $\delta = 0$, the expression for $K_{ij}(0)$ coincides with with the sum in the first term. The expression for A_{ij} in polynomial approximation is

$$A_{ij} \approx \{[\theta(t_j + \delta) - \theta(t_{j-1} + \delta)] S_j + \sum_{\lambda=1}^{m} a_{j\lambda} [\theta(t_j + \delta)(h + \delta)^\lambda - \theta(t_{j-1} + \delta)\delta^\lambda]\} I_{ij} \tag{26}$$

$$I_{ij} = \int_0^h I(x + t_{i-1} - t_j) dx \tag{27}$$

Direct analysis of Eqs. 25–27 shows that for the linear approximation ($m = 1$) and $\delta > 0$, the expression for F_i does not depend on δ. The consequence of that is quite remarkable, namely, that linear approximation will be substantially inaccurate when the zero-time shift is larger than, or of an order of, one channel.

The coefficients a_{jl} can be determined from Eqs. 23, 7, and 9, yielding

$$\sum_{\lambda=1}^{m} a_{j\lambda} (1 + \kappa)^\lambda h^\lambda = \sum_{\nu=0}^{\kappa} R_{j+\nu}, \qquad j = 1, \ldots, n, \quad \kappa = 0, 1, \ldots, n - j, \tag{28}$$

$$\sum_{\lambda=1}^{m} a_{j\lambda} (1 - \kappa)^\lambda h^\lambda = -\sum_{\nu=1}^{\kappa-1} R_{j-\kappa+\nu}, \quad j = 2, \ldots, n, \quad \kappa = 2, \ldots, j. \tag{29}$$

It is important to realize that for $m > 1$ we have more equations than unknowns, a_{jl}. Thus, by choosing different sets of m equations, we obtain different polynomial approximations of a given order and for a given j. In Table 1, we present coefficients for linear (LA), two quadratic (Q1, Q2), and three cubic (C1, C2, C3) approximations of $\rho_j(t)$, whereas in Fig. 1 these approximations are illustrated visually.

When the polynomial approximation given by Eq. 23 is applied to the case of the multiexponential decay model, Eqs. 21 and 22 specialize to a computationally convenient iterative form:

$$F_i^k = D_k F_{i-1}^k + \Delta_{ik}^m(\delta), \quad i = 1, \ldots, n, \quad F_0^k = 0 \tag{30}$$

$$\Delta_{ik}^m(0) = A_k h \sum_{\lambda=0}^{m} c_{i\lambda} Z_\lambda, \quad c_{i0} = R_{i-1}, \quad c_{0\lambda} \equiv 0, \quad c_{i\lambda} = (a_{i\lambda} - a_{i-1\lambda}) h^\lambda, \tag{31}$$

$$Z_\lambda = p_k^{-1}(1 - l Z_{\lambda-1}), \quad \lambda = 1, \ldots, m, \qquad Z_0 = (1 - D_k) p_k^{-1}, \quad p_k = h/\tau_k. \tag{32}$$

TABLE 1 Coefficients for linear, quadratic, and cubic approximations

m	Approx.	Eq.	κ	l	$b_{il} = a_{il}h^l$	$i = 1, 2, n-1, n$
1	LA	(28)	0	1	R_i	
2	Q1	(28)	0	1	$(3R_i - R_{i+1})/2$	b_{nl}(Q2)
		(28)	1	2	$(-R_i + R_{i+1})/2$	
	Q2	(28)	0	1	$(R_{i-1} + R_i)/2$	b_{1l}(Q1)
		(29)	2	2	$(-R_{i-1} + R_i)/2$	
3	C1	(28)	0	1	$(-R_i - 7R_{i+1} + 2R_{i+2})/6$	b_{n-1l}(C2)
		(28)	1	2	$(-2R_i + 3R_{i+1} - R_{i+2})/2$	b_{nl}(C3)
		(28)	2	3	$(R_i - 2R_{i+1} + R_{i+2})/6$	
	C2	(28)	0	1	$(2R_{i-1} + 5R_i - R_{i+1})/6$	b_{1l}(C1)
		(28)	1	2	$(-R_{i-1} + R_i)/2$	b_{nl}(C3)
		(29)	2	3	$(R_{i-1} - 2R_i + R_{i+1})/6$	
	C3	(28)	0	1	$(-R_{i-2} + 5R_{i-1} + 2R_i)/6$	b_{1l}(C1)
		(29)	2	2	$(-R_{i-1} + R_i)/2$	b_{2l}(C2)
		(29)	3	3	$(R_{i-2} - 2R_{i-1} + R_{i-2})/6$	

Notation is explained in the text. In the last column, the coefficients that are not given in the preceding column are designated with the symbol corresponding to approximation that allows their calculation from IRF data $R_1, \ldots, R_n$.

The expression for $\Delta_{ik}(\delta)$, $\delta \neq 0$ is rather cumbersome and is explicitly given in the Appendix. The above expression for Z_λ is iterative and, therefore, computationally convenient. However, Z_λ can be also written as a polynomial in $1/p_k$:

$$Z_\lambda = \sum_{\mu=1}^{\lambda+1} (-1)^{\lambda+\mu+1} \frac{\lambda!}{(\mu-1)!} \frac{1 - \delta_{\lambda-\mu+1\lambda} D_k}{p_k^{\lambda-\mu+2}}. \quad (33)$$

With this form of Z_λ, Eq. 33 resembles the equivalent equation of Večeř et al. (1993) (see Eq. 4 of their paper). Moreover, for the linear approximation (LA, Table1) with

$$\rho_j^1(x) = (x - t_{j-1})R_j/h \quad (34)$$

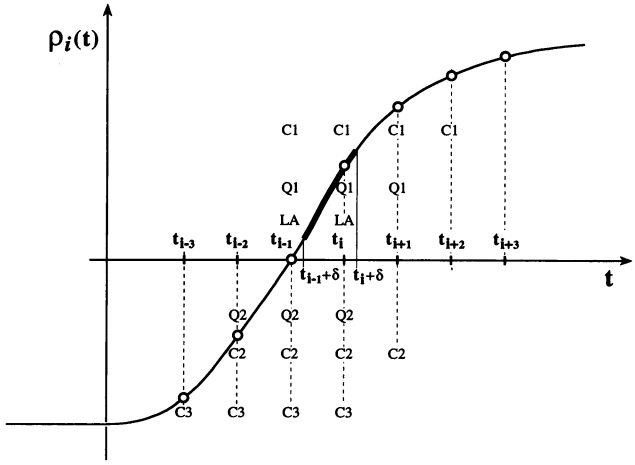

FIGURE 1 Count function for channel i and its polynomial approximations. Thicker line segment illustrates the part of $\rho_i(t)$, which has to be approximated when a small positive zero time shift δ is included. Above or below each knot t_j, $j = i-3, i-2, \ldots, i+2$ the symbols corresponding to various polynomial approximations given in Table 1 are displayed to indicate those knots that are included in a given approximation. Note that according to Eq. 6 for $t \leq 0$ the count function is a negative constant.

our formula (Eqs. 20–33) is identical to that of Večeř et al. (1993) for their linear approximation, i.e., $\Delta_{ik}^1(0)/h \equiv \Delta F_{ik}^{(1)}$. At first, this identity appears paradoxical because, as we have pointed out earlier, there is a substantial difference between the two approaches. However, because we approximated the function $\rho_j(x)$ by linear approximation, and Večeř et al. (1993) approximated the function $R(t)$ by linear approximation, the difference in final formulae disappears. In other words, our linear approximation of $\rho_j(t)$ corresponds to the constant approximation of $R(t)$ by Večeř et al. but, interestingly enough, the inherently more powerful discretization formula (Eqs. 20–22) brings us to the same final result. Our LA formula also agrees with the formula presented by Wahl (1979) for all F_i, except for F_1, which he treated separately. Quite surprisingly, our LA formula agrees with that proposed by McKinnon et al. (1977) (see Supplementary Material of that paper) and later reinvented by Periasamy (1988). In these two papers, the initial model for F_i is not the one given by Eq. 1 but, rather, by $F_i = \int_0^{(i-1)h} R(u)I((i-1)h - u)du$. Also, in their approach IRF counts R_i were treated in a different way than in the present paper (cf. Bajzer and Prendergast 1992).

For the quadratic approximation ($m = 2$, Q1 of Table 1):

$$\rho_j^2(x) = [(R_{j+1} - R_j)h^{-2}(x - t_{j-1})^2 + (3R_j - R_{j+1})h^{-1}(x - t_{j-1})]/2, \quad (35)$$

we found that our formula is identical to that of Holtom (1990) and Večeř et al. (1993) (i.e., $\Delta_{ik}^2(0)/h \equiv \Delta F_{ik}^{(2)}$.

Our cubic approximation C1 from Table 1 can be compared with the cubic approximation given by Večeř et al. (1993) because both contain the same set of IRF counts, namely, R_{i+2}, R_{i+1}, R_i, R_{i-1}. However, these two cubic approximations do not lead to the same discretization formula as was found for the quadratic and the linear approximations. Thus, the difference in the two approaches affects the discretization formula for multiexponential decay and

for the polynomial approximation at the level of a third-order polynomial.

We conclude this paragraph with a comment derived from elementary approximation theory. The higher order polynomial approximation $\rho_i^m(t)$ certainly will provide better approximation for $\rho_i(t)$ and, consequently, for F_i. However, this is not necessarily true when $\rho_i(t_i) = R_i$ is noisy. Therefore, we are bound to take the noise into consideration, and this can be achieved by simulations.

DATA SIMULATIONS AND ANALYSIS

The relevance of higher polynomial approximations to the accuracy of fluorescence decay parameter recovery was tested by means of simulated fluorescence decay data. For this purpose, we used an analytical IRF function of the form (see O'Connor and Phillips, 1984):

$$R(t) = \alpha t^2 e^{-\beta t} \tag{36}$$

where α is determined to yield required full-width at half-maximum (*FWHM*) and β is determined so that $\max_i R_i = C$, where C is the given number of counts in a peak channel, which reflects signal-to-noise ratio.

Fluorescence intensity counts f_i were calculated from Eqs. 1, 2, and 36 with the multiexponential decay function of Eq. 19, given zero-time shift δ, given scattering parameter ξ, and given the background constant $b = 0.0001C$. The scaling was chosen to yield given number of counts in a peak channel (i.e., $\max_i f_i = C$.) The Poisson noise was added, both to f_i and R_i.

The synthetic noisy data were analyzed by the maximum likelihood method (Bajzer et al., 1991; Bajzer and Prendergast, 1992), which requires minimization of the Poisson deviance:

$$D = 2\sum_{i=1}^{n}[c_i \ln(c_i/f_i) - c_i + f_i] \tag{37}$$

with respect to model parameters. Here c_i are "measured" counts of the fluorescence intensity profile and f_i is the model function depending on model parameters. Theoretically, this function is given by Eq. 1. However, for actual evaluation of this function it is necessary to use its discretized form (Eqs. 1, 20, 30, and 43–47), which includes IRF counts R_i. These can only be obtained by measurements and are necessarily corrupted by noise. Therefore, to make our simulations realistic, the Poisson noise was added to IRF counts calculated from Eqs. 2 and 36. (The expression presented for the deviance does not take into account the fact that f_i in discretized form contains noisy IRF counts. To derive a rigorous expression for deviance with noise and IRF counts considered would require substantial theoretical development, and our simulations (see Recovery of Short Lifetimes for Two-Component Decays) do not indicate that the effects of that noise significantly change the accuracy of parameter estimation.)

At minimum D is theoretically distributed as χ^2 distribution with $\nu = n - 2N - 3$ degrees of freedom (cf. Bajzer and Prendergast, 1992) and, therefore, we will use notation $D_{min}/\nu = \chi^2_\nu$. To estimate the goodness of fit, we use the standard normal variate $Z = \nu(\chi^2_\nu - 1)/(2\nu)^{1/2}$. For an acceptable fit (cf. O'Connor and Phillips, 1984), $|Z|$ should be <3 with 0.997 probability.

The Poisson deviance was minimized using the modified Levenberg-Marquardt algorithm (More, 1977) implemented in a finely tuned subroutine that calculates derivatives numerically (Morris, 1981). When in some occasions this algorithm yielded unreliable results, we used the more robust (but not fast) Nelder-Mead simplex algorithm (Press et al., 1986). All calculations were performed in double precision.

For each intensity profile, we used three different polynomial approximations for discretization: linear (LA), quadratic (QA), and cubic (CA). The quadratic approximation was a combination of Q1 and Q2, namely, for $\delta \geq 0$ we used Q1, and for $\delta < 0$ we used Q2. Similarly, the cubic approximation was a combination of C1 (for $\delta \geq 0$) and C3 (for $\delta < 0$). Such a strategy was adopted as an optimal solution based on preliminary synthetic data analyses in which all possible approximations displayed in Table 1 were separately attempted for negative and positive zero-time shifts. Fig. 1 also clearly indicates that approximations Q1 and C1 will be more accurate for positive zero-time shifts, whereas the approximations Q2 and C3 will be more accurate for negative time shifts. It is noteworthy that during the process of minimization of the Poisson deviance the intensity profile counts are calculated in an adaptive fashion, i.e., with, say, Q1 or Q2 depending on whether the current value of the zero-time shift is positive or negative. In our preliminary studies, we found that the relative error of approximation for channel i: $e_i = |F_i - F_i^{approx}|/F_i$ is most often significantly larger in two among initial channels than in all other channels. Therefore, we sort all e_i by its magnitude, obtaining e_j^s, $j = 1, \ldots, n$, and characterize the overall approximation error by three numbers:

$$e_1^{max} = e_1^s, \qquad e_2^{max} = e_2^s, \qquad \bar{e} = \frac{1}{n-2}\sum_{j=3}^{n} e_j^s. \tag{38}$$

The final goal of fluorescence intensity data analysis involving the multiexponential decay is the recovery of decay parameters: lifetimes τ_k and corresponding amplitudes A_k. Therefore, the success of a given discretization scheme in data analysis should be measured by accuracy achieved in determining those parameters. In the case of many various simulations, it would be difficult to compare accuracy for all parameters separately. Therefore, we used the average relative error per parameter defined as (cf. Eisenfeld and Ford, 1979; Bajzer et al., 1990):

$$E = \frac{1}{N}\sum_{k=1}^{N}[|\tau_k - \tau_k'|/\tau_k + |A_k - A_k'|/A_k] \tag{39}$$

where τ_l' are estimated lifetimes and A_l' corresponding estimated amplitudes. The index l is such that for a given k, the absolute difference $|\tau_k - \tau_l'|$ is minimal.

To account for noise fluctuations for each set of parameters, each IRF, and each discretization, we analyzed 101 synthetic data that differed only by added Poisson noise. After parameter recoveries, we determined corresponding average relative errors E and calculated the median of these errors, E_{med}. This quantity was used to measure the success of a specific discretization. The three approximations, LA, QA and CA, were compared by use of E_{med}, and from these data we were able to make inferences.

Another criteria for comparison we will use are the coefficient of variation, CV, and the relative bias, RB, of any decay parameter p defined as: $CV(p) = SD(p)/\bar{p}$, $RB(p) = |p - \bar{p}|/p$, where $\bar{p}$ and $SD(p)$ are the estimated mean value (from 101 data) and the estimated SD, respectively.

RESULTS OF SIMULATIONS AND DISCUSSION

Comparison with literature data

In the studies of Periasamy (1988) and Večeř et al. (1993), a number of selected simulations were performed to assess the relative merit of different discretization formulae for the multiexponential decay model. Here we will take the same path, but first we compare some simulations from these studies with corresponding simulations based on our approach.

In Table 2, we compare results of simulations for two different sets of amplitudes and lifetimes with Periasamy's and our linear approximation. The agreement is excellent despite some differences in the simulation of R_i (cf. Bajzer and Prendergast, 1992) and the difference in F_1 which Periasamy approximated by $hR_1(A_1 + A_2)$, where A_1 and A_2 are the amplitudes in the two-exponential decay (see Eq. 19). The fact that we used the maximum likelihood method to analyze data corrupted by Poisson noise and he used the weighted least-squares method to analyze the data corrupted by the Gaussian noise in theory should not matter. As for the results themselves, Table 2 shows that a reasonably accurate estimation of a lifetime τ_1, shorter than the channel width, might be possible if A_1/A_2 is sufficiently large.

In Table 3, we compare results of simulations for linear, quadratic, and cubic approximation as given by Večeř et al. (1993) and by our approach. The corresponding results agree well within the estimated uncertainties. Because the corresponding discretization formulae are identical for linear and quadratic approximation, significant differences between our and their estimated parameter values could theoretically emerge: 1) from somewhat different treatment of background counts, and 2) from the fact that we applied the maximum likelihood method to data corrupted by the Poisson noise while they applied the weighted least-squares method to data corrupted by Gaussian (for number of counts >100) and Poisson noise (for number of counts <100). However, the effects of these differences appear to be insignificant. The same is true for the cubic approximation where the actual differences in discretization formulae exist.

Apart from comparison, the results presented in Table 3 show again that fairly accurate parameter estimation can be achieved even when the short lifetime is 5 times shorter than the channel width. This is possible apparently because the amplitude of the short lifetime is 10 times larger than the amplitude of the long lifetime. Another interesting fact that Table 3 reveals is that the estimated parameters for linear, quadratic, and cubic approximations are all equal within the

TABLE 3 Comparison of results for present simulations and those of Večeř et al. (1993)

	Reference	Linear	Quadratic	Cubic
χ^2_ν	VKD-93	1.325	1.246	1.250
	this work	1.296	1.281	1.316
A_1: 0.0909	VKD-93	0.0923 (70)	0.1013 (81)	0.0976 (85)
	this work	0.0918 (64)	0.0991 (84)	0.0946 (97)
τ_1: 1.0	VKD-93	1.021 (14)	1.014 (14)	1.011 (13)
	thiswork	1.012 (17)	1.005 (16)	1.002 (16)
A_2: 0.9091	VKD-93	0.9077 (70)	0.8987 (81)	0.9023 (85)
	this work	0.9082 (64)	0.9009 (84)	0.9054 (97)
τ_2: 0.1	VKD-93	0.122 (11)	0.125 (12)	0.116 (13)
	this work	0.116 (15)	0.116 (17)	0.106 (18)
h = 0.5 ns; 21 channels, first 2 excluded, noisy data				

The reference VKD-93 denotes Večeř et al. (1993), and the data were taken from Table 6 of that paper. The IRF used is given by Eq. 11 of VKD-93 with the following characteristics: $FWHM$ = 2.46 ns, $C = 6 \times 10^4$ counts. The background constant for "this work" was b = 6 counts. The amplitudes were normalized to 1. The lifetimes are given in nanoseconds. The parameter values and the χ^2_ν of this work are mean values resulting from 101 synthetic data sets, whereas the corresponding values of VKD-93 resulted from the analysis of one data set. The numbers in parenthesis are the first two nonzero digits of the corresponding SDs, for example, 0.116 (15) means 0.116 ± 0.015. In this work, the SDs were estimated from the values of parameters obtained in 101 analyses, whereas in VKD-93 the SDs were estimated from the covariance matrix.

TABLE 2 Comparison of results for present and previous simulations

A_1; τ_1; A_2; τ_2	Reference	$FWHM$	$(A_1/A_2)'$	τ_1'	$(\chi^2_\nu)'$
10; 0.02; 1; 1	Periasamy (1988)	0.65	8.56 ± 0.19	0.024 ± 0.001	1.27 ± 0.16
	this work		8.58 ± 0.27	0.024 ± 0.001	1.18 ± 0.08
1; 0.02; 1; 1	Periasamy (1988)	0.35	0.52 ± 0.03	0.040 ± 0.003	1.26 ± 0.15
	this work		0.51 ± 0.03	0.042 ± 0.003	1.32 ± 0.06
h = 0.05 ns; 512 channels; IRF: Eq. 34, $C = 10^5$ counts; 10 noisy data sets; b = 0.					

The data were taken from the Table 3 of Periasamy's paper. The values of lifetimes and $FWHM$ are expressed in nanoseconds. Notation as in text; the quantities denoted by prim designate estimated average values and the corresponding SDs.

uncertainty of 1 SD. However, the relative bias for both lifetimes, $RB(\tau_i)$, $i = 1, 2$, is clearly smaller when the cubic approximation is applied.

The consistency achieved between our simulations and those from literature increases our confidence in results so far obtained. Now we can proceed to more ambitious investigations, namely, to approach the questions of interest to researchers in the field to wit: What is the shortest lifetime we can safely recover (other parameters and experimental conditions being given), and are any of the polynomial approximations for discretization to be preferred?

Recovery of short lifetimes for two-component decays

Our strategy is to search for the shortest possible lifetime that can be recovered with prescribed minimal accuracy for all of the decay parameters. In our simulations, we lower the value of the shortest lifetime until one of the coefficients of variation of decay parameters reaches a value between 14 and 16% and E_{med} is not larger than 0.16 or until E_{med} is between 0.14 and 0.16 and none of coefficients of variations of decay parameters exceeds 16%. We chose experimental conditions commonly found in our laboratory: the width of IRF is $FWHM = 0.1$ ns, $h = 0.01$ ns, $C = 2 \times 10^4$ counts. The value of light scattering parameter is chosen to be $\xi = 0.1$ if not otherwise stated. For the case of any of the parameters δ and/or ξ chosen to be zero, we assume that this is an a priori information and do not perform minimization with respect to these parameters. Similarly, for the case of $\delta > 0$ the linear approximation is equivalent to assuming $\delta = 0$ and, therefore, the minimization with respect to this parameter is omitted. The result of such a procedure is advantageous for the linear approximation and, consequently, does not hinder our final conclusion of its relative inadequacy.

Under such conditions and $A_1/A_2 = 10$ where $A_1 = 0.909$ is the normalized amplitude of the shorter lifetime, we found that the shortest lifetime is ~5 times shorter than the channel width for QA and CA and ~3.4 times shorter for LA (Table 4, $\delta = 0$, $\xi = 0$). The criteria for approximation error e_1^{max}, e_2^{max}, and $\bar{e}$ show consistent decrease when higher polynomial approximation is applied, as one would expect. However, this decrease does not help CA to yield significantly better recovery of decay parameters than QA. If anything is different between QA and CA, the biases $RB(A_1)$ and $RB(A_2)$ are slightly smaller for CA. The bias for all parameters when LA is applied is significantly larger than for QA and CA, and the limiting error for LA is E_{med}, whereas for QA and CA this is $CV(\tau_1)$. In summary, these data clearly suggest that LA is inferior to QA and CA, whereas there is no marked preference between these two discretization approximations, which are both capable of extending our ability to determine short lifetimes.

When the light-scattering parameter is not zero ($\xi = 0.1$), we observe that the shortest recoverable lifetime increases significantly from the case $\xi = 0$ (Table 4), but otherwise the behavior with respect to different approximations remains the same. The significant increase is also seen for approximation error $\bar{e}$, but not for e_1^{max} and e_2^{max}.

This picture remains similar when more realistic data with $\delta = 0.8h$ and $\xi = 0.1$ are synthesized, except that now our ability to recover short lifetimes is greatly reduced, which appears to be a consequence of a larger approximation error $\bar{e}$. QA and CA still yield practically the same result with $\tau_1 = 1.6h$, whereas when LA is applied to the same data we can recover only $\tau_1 = 3h$. Surprisingly different results are obtained for the negative zero-time shift, $\delta = -0.8h$. Here all three approximations yield shortest recoverable lifetime of $\sim h/2$, but the relative bias for all parameters recovered when LA is applied is much larger

TABLE 4 The shortest recoverable lifetime when its corresponding amplitude is large

PA	τ_1	$\bar{\tau}_1$	$CV(\tau_1)$%	$\bar{A}_2$	$CV(A_2)$%	E_{med}*	e_1^{max}	e_2^{max}	$\bar{e}$
				$\tau_2 = 1000$, $A_1 = 10\,A_2$, $A_2 = 0.0909$, $\delta = 0$, $\xi = 0$					
LA	2.90	3.8	7.4	0.114	6.2	0.144 (6)	0.480	0.059	$3.2 \cdot 10^{-4}$
QA	2.10	1.8	14.3	0.080	12.9	0.070 (6)	0.170	0.014	$3.9 \cdot 10^{-5}$
CA	2.05	1.8	14.4	0.080	12.8	0.064 (6)	0.118	0.002	$2.2 \cdot 10^{-5}$
				$\delta = 0$, $\xi = 0.1$					
LA	10.5	8.4	6.1	0.061	9.8	0.144 (4)	0.428	0.066	$1.6 \cdot 10^{-3}$
QA	5.6	6.8	9.9	0.123	14.1	0.15 (1)	0.172	0.017	$1.5 \cdot 10^{-4}$
CA	5.6	10.9	10.9	0.114	15.8	0.102 (9)	0.122	0.004	$2.6 \cdot 10^{-5}$
				$\delta = 8$ $\delta_L = 0$ $\delta_Q = 7.3$ (5)* $\delta_C = 7.6$ (5)					
LA	30.0	32.4	2.0	0.133	2.6	0.146 (2)	0.589	0.454	$2.4 \cdot 10^{-2}$
QA	16.0	16.1	7.9	0.100	14.9	0.054 (5)	0.068	0.008	$1.4 \cdot 10^{-3}$
CA	16.0	16.1	7.7	0.095	15.7	0.047 (4)	0.040	0.009	$4.3 \cdot 10^{-4}$
				$\delta = -8$ $\delta_L = -0.0$ (5) $\delta_Q = -8.2$ (7) $\delta_C = -8.1$ (7)					
LA	5.5	7.7	6.0	0.075	9.0	0.1471 (4)	1.470	0.708	$9.2 \cdot 10^{-3}$
QA	5.0	4.9	14.4	0.090	13.5	0.040 (6)	0.017	0.016	$5.4 \cdot 10^{-4}$
CA	5.0	5.0	14.4	0.091	13.6	0.043 (6)	0.012	0.007	$1.2 \cdot 10^{-4}$

The symbols and the accuracy criteria are explained in the text. $\bar{\tau}_1$ and $\bar{A}_2$ designate the estimated mean values from 101 fits. The values of lifetimes and zero time shift are expressed in picoseconds. $h = 10$ ps, $n = 512$ channels, $FWHM = 100$ ps, $C = 2 \cdot 10^4$ counts.

* The number in parentheses is the first nonzero digit of the corresponding SD.

than for QA or CA. The approximation errors follow the same pattern as before, e_1^{max}, e_2^{max}, and $\bar{e}$ having the greatest values for LA. However, the approximation errors for $\delta = -0.8h$ are consistently smaller then those for $\delta = 0.8h$. What is the cause of such asymmetry? One answer may come from the possibility that the "count function" $\rho_i(t)$, $i > 1$, is best approximated by the polynomial (Eq. 23) around its zero at $t = t_{i-1}$, $i > 1$, and for $\delta < 0$, $\delta > -h$ the point t_{i-1} is included in the approximation interval, whereas for $\delta > 0$ this does not happen (see Fig. 1).

In Table 4 we have also displayed the result of estimation of the zero-time shift, although in the final analysis this parameter is not important for data interpretation. However, the estimation of δ reveals the internal consistency of the discretization applied. In the case of $\delta = 0.8h$ and with LA, the considerations above (see also third paragraph in Introduction) provide theoretical result $\delta_L = 0$, whereas for quadratic and cubic approximations the corresponding estimated mean values δ_Q and δ_C are both fairly close to the true value. For $\delta = -0.8h$, the minimization yielded zero mean value δ_L to three significant digits. The mean value estimates δ_Q and δ_C again are insignificantly different and close to the true value.

So far we have not discussed the goodness-of-fit criterion introduced in the previous section. For all but one of the presented fits, there were always all 101 or 100 data sets for which $|Z| < 3$ (or $0.81 < \chi_\nu^2 < 1.19$), which is consistent with the corresponding theoretical probability. The only exception were the fits for LA with $\delta = 0.8h$ when 90 of 101 fits satisfied $|Z| < 3$, which is a clear sign that applied discretization produces significant systematic errors (larger than noise). This, of course, is consistent with a high value of approximation error $\bar{e}$.

The question now arises to what extent can the essence of results presented in Table 4 be reproduced when amplitudes are equal. First, it is clear from Table 5 that our ability to recover short lifetime when $\delta = 0$ or $\delta = -0.8h$ significantly deteriorated in comparison with the case of $A_1/A_2 = 10$. Interestingly, this is much less pronounced for $\delta = 0.8h$, where a relatively small increase of the shortest recoverable lifetime is observed. Concerning the approximation errors, the pattern remains the same as in Table 4, but the magnitudes do not reflect consistently the ability for short lifetime recovery. For example, $\bar{e}$ for LA and $\delta = 0$, $\xi = 0$ is even smaller in Table 5 than in Table 4.

New features in Table 5 appear for larger negative zero-time shifts. For LA and $\delta = \pm 1.6h$ there is no above mentioned asymmetry; however, it is still present for QA and CA. Another feature is the significant difference between the LA and higher order approximations and clear advantage of CA over QA for $\delta = -2.6h$. Such behavior of different approximations for various zero-time shifts is illustrated in Fig. 2. Cubic approximation is certainly most advantageous when the zero-time is shifted for more than one channel. From this figure, we also observe asymmetry in accuracy with respect to negative and positive shifts and the fact that for the positive shifts QA and CA start to differ significantly for larger $|\delta|$ than for the negative shifts. All of this suggests that if any zero-time shift is expected we certainly can achieve better accuracy in estimated parameters if we use the cubic approximation.

TABLE 5 The shortest recoverable lifetime when the amplitudes are equal

PA	τ_1	$\bar{\tau}_1$	$CV(\tau_1)$	$\bar{A}_1$	$CV(A_1)$	E_{med}	e_1^{max}	e_2^{max}	$\bar{e}$
				$\tau_2 = 1000$, $A_1 = A_2 = 0.5$, $\delta = 0$, $\xi = 0.1$					
LA	17.0	13.7	11.6	0.60	7.3	0.154 (8)	0.276	0.061	$2.8 \cdot 10^{-4}$
QA	11.7	13.6	14.6	0.44	12.0	0.102 (9)	0.129	0.017	$3.8 \cdot 10^{-5}$
CA	11.7	13.1	15.5	0.46	12.6	0.089 (9)	0.092	0.002	$5.7 \cdot 10^{-6}$
				$\delta = 8$ $\delta_L = 0$ $\delta_Q = 6.9$ (8) $\delta_C = 7.4$ (8)					
LA	35.0	39.9	5.2	0.38	4.2	0.150 (4)	0.524	0.411	$1.2 \cdot 10^{-2}$
QA	20.0	20.4	15.0	0.48	15.1	0.073 (7)	0.060	0.009	$3.3 \cdot 10^{-4}$
CA	20.0	20.4	14.8	0.49	15.2	0.078 (8)	0.036	0.009	$3.2 \cdot 10^{-5}$
				$\delta = -8$ $\delta_L = -0$ (2) $\delta_Q = -9$ (1) $\delta_C = -8$ (1)					
LA	12.8	17.9	8.5	0.45	6.7	0.153 (7)	0.665	0.562	$1.0 \cdot 10^{-2}$
QA	14.7	14.0	15.0	0.52	8.5	0.057 (7)	0.022	0.009	$3.2 \cdot 10^{-4}$
CA	15.1	14.9	15.5	0.51	9.8	0.057 (7)	0.016	0.004	$3.5 \cdot 10^{-5}$
				$\delta = 16$ $\delta_L = 0$ $\delta_Q = 19$ (2) $\delta_C = 16$ (1)					
LA	73.0	86.2	2.5	0.39	1.7	0.154 (2)	0.733	0.598	$2.9 \cdot 10^{-2}$
QA	25.5	28.9	14.8	0.48	15.7	0.077 (9)	0.056	0.032	$3.4 \cdot 10^{-3}$
CA	25.5	25.6	14.0	0.51	14.8	0.067 (8)	0.018	0.009	$1.2 \cdot 10^{-4}$
				$\delta = -16$ $\delta_L = -18$ (2) $\delta_Q = 15.2$ (8) $\delta_C = -16$ (1)					
LA	113	152	4.6	0.44	3.4	0.155 (1)	0.615	0.572	$3.1 \cdot 10^{-2}$
QA	13.5	16.9	12.1	0.41	8.2	0.145 (9)	0.049	0.027	$1.6 \cdot 10^{-3}$
CA	14.3	14.4	15.1	0.50	9.4	0.055 (6)	0.008	0.005	$5.1 \cdot 10^{-5}$
				$\delta = -26$ $\delta_L = -21$ (6) $\delta_Q = -20$ (10) $\delta_C = -24.6$ (6)					
LA	220	318	6.2	0.47	0.7	0.155 (3)	0.622	0.566	$3.7 \cdot 10^{-2}$
QA	75.5	94.0	6.5	0.44	6.2	0.144 (5)	0.177	0.159	$1.3 \cdot 10^{-2}$
CA	13.0	15.5	15.1	0.43	10.5	0.116 (9)	0.067	0.050	$2.4 \cdot 10^{-4}$

Notation and measurement parameters as in Table 4.

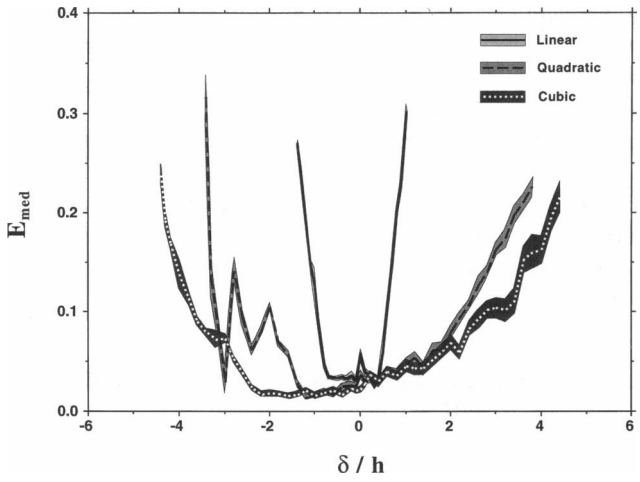

FIGURE 2 Accuracy of decay parameter estimation for the linear, quadratic, and cubic approximations as a function of the zero-time shift. The accuracy is represented by the median of the average relative error in parameters E_{med} (Eq. 39) and the respective SD illustrated by shaded areas. Fluorescence intensity decay curves were synthesized based on: $n = 512$ channels, $C = 2 \times 10^4$ counts, $h = 10$ ps, $FWHM = 100$ ps, $\tau_1 = 30$ ps, $\tau_2 = 1000$ ps, $A_1 = A_2 = 0.5$, $\xi = 0.1$, $b = 2$ counts.

It is interesting to note that the goodness-of-fit criterion for the results in Table 5 definitely was violated only for LA with zero-time shifts of $\pm 1.6h$ and LA and QA for $\delta = -2.6h$. There was no single fit for LA with $|Z| < 3$, and χ^2_ν was generally greater than 3, for $\delta = -1.6h$, than 1.3 for $\delta = 1.6h$ and greater than 3.8 for $\delta = -2.6h$. For QA and $\delta = -2.6h$ the criterion $|Z| < 3$ was satisfied only for 21 of 101 data sets, with χ^2_ν generally greater than 2. Such high χ^2_ν values are reflected in higher relative biases, which reach 0.3. In practice, the fits with so high a χ^2_ν would be rejected and the fit on a model with more exponential components would be attempted, possibly yielding a much more acceptable fit. This may represent a danger for correct data interpretation, and it might be more acceptable to rely on two-exponential decay with somewhat inaccurately determined parameters than to introduce another decay component. However, the problem at this level of zero-time shift disappears completely if we use the cubic approximation.

The question arises whether the cubic and quadratic approximations are still advantageous in the case of much smaller signal-to-noise ratios, which we characterize with C—the number of counts in the peak channel. In this case, the noise may mask the error of discretization. Indeed, from Table 6 it is clear that the advantage of QA and CA over LA gradually disappears. Thus, for C as low as 200–400 counts, although QA and CA are advantageous compared with LA with respect to the relative bias in τ_1 and A_2, there is a clear disadvantage of QA and CA because of unacceptably large coefficient of variation in A_2. However, for $C = 2000$ QA and CA have to be considered advantageous for parameter estimation because of the very small biases and acceptable coefficients of variations.

The effect of noise in IRF counts appears to be insignificant. We came to this conclusion comparing the results of simulations for which R_i involved in discretization formula was first noisy and then without noise. An example of such

TABLE 6 The accuracy of lifetimes and amplitudes recovery for decreasing number of counts in the peak channel

PA	$\bar{\tau}_1$	$CV(\tau_1)\%$	$RB(\tau_1)\%$	$\bar{A}_2$	$CV(A_2)\%$	$RB(A_2)\%$	E_{med}	δ
				$C = 20000$				
LA	32.4	2.0	8.0	0.133	2.6	46.3	0.146 (2)	0
QA	30.1	2.5	0.3	0.095	5.3	4.5	0.017 (2)	7.1 (6)
CA	30.0	2.5	0.0	0.092	5.5	1.2	0.015 (2)	7.6 (6)
				$C = 10000$				
LA	32.3	2.8	7.7	0.133	3.7	46.3	0.147 (3)	0
QA	30.0	3.3	0.0	0.095	7.3	4.5	0.018 (2)	7.1 (8)
CA	30.0	3.4	0.0	0.092	7.4	1.2	0.015 (2)	7.6 (8)
				$C = 2000$				
LA	32.3	6.1	7.7	0.131	7.9	44.1	0.142 (5)	0
QA	29.6	6.5	1.3	0.092	14.7	1.2	0.037 (4)	7 (2)
CA	29.6	6.6	1.3	0.090	14.7	1.0	0.036 (4)	8 (2)
				$C = 400$				
LA	32.1	13.0	7.0	0.132	16.3	45.2	0.14 (1)	0
QA	29.1	13.9	3.0	0.087	28.4	4.3	0.087 (7)	8 (4)
CA	29.1	13.7	3.0	0.087	28.6	4.3	0.084 (7)	8 (4)
				$C = 200$				
LA	32.7	22.7	9.0	0.134	27.7	47.4	0.16 (2)	0
QA	29.4	23.6	2.0	0.086	37.1	5.4	0.12 (1)	9 (5)
CA	29.5	22.9	1.6	0.086	35.9	5.4	0.12 (1)	9 (4)
				$C = 200$ noiseless R_i				
LA	32.9	19.1	9.6	0.134	23.6	47.4	0.17 (2)	0
QA	30.5	20.3	1.7	0.099	35.0	8.9	0.12 (1)	6 (4)
CA	30.3	20.8	1.0	0.098	36.1	7.8	0.12 (1)	6 (5)

The symbols and the accuracy criteria are explained in the text and in Table 4. Here $\tau_1 = 30$ ps, $A_1 = 10\,A_2$, $A_2 = 0.0909$, $\delta = 8$ ps, $h = 10$ ps, $n = 512$ channels, $FWHM = 100$ ps.

comparison is furnished by two last triplets of results in Table 6 ($C = 200$).

Recovery of short lifetimes for three-component decays

Neither Periasamy (1988) nor Večeř et al. (1993) presented simulations of heterogeneous decays with more than two lifetimes. Here we have selected some three-component decays to illustrate how different discretization approximations perform in such more complicated circumstances (Table 7). In the case that the amplitude of the shortest lifetime is 10 times larger than the other two, we observe a slight increase in the shortest recoverable lifetime compared with the similar two-component decay (compare second triple of simulations in Table 4 with the first triple in Table 7). The quadratic and cubic approximations are still much more effective than linear approximation. However, the next more difficult example of Table 7 shows that all three approximations are equally poor in recovering a short lifetime with corresponding amplitude 4 times smaller than the other two and $\delta = 0.8h$. When the zero-time shift becomes $\delta = -2.4h$ (Table 7), we encounter the situation that only the cubic approximation can provide recovery of parameters within given accuracy. Neither LA and QA meets the accuracy criteria as we change τ_1. The values of τ_1 higher than 160 ps become already too close to the value of τ_2, so that the accuracy is lost because of closely spaced lifetimes.

The results presented for three-component decay with $\delta \neq 0$ are noteworthy. Researchers might view recoveries of a 10-ps lifetime with great caution, but may *not* pay special attention to recoveries of lifetimes of the order of 100 or more ps. Yet, as our examples show, such "long" lifetimes may be at the limit of acceptably accurate recovery. Remedy to that possibility can be found by increasing the signal-to-noise ratio, decreasing the channel width, and increasing the number of channels. The last example of Table 7 shows that we can recover lifetimes shorter than 100 ps in the three-component decay example, considered above, for $\delta = 0.8h$ if we double the number of channels and the number of counts in the peak channel and reduce the channel width by half. In that case, QA and CA again become preferable over LA, although the approximation errors for QA or CA have not decreased relatively with respect to approximation errors for LA. The effect, therefore, should be attributed to the increased information content in the data and some details of discretization to which our characterization of approximation error is not sensitive.

Dependence on the width of the instrument response function

It is generally believed that one's ability to estimate decay parameters accurately increases as the width of IRF decreases. We performed a number of simulations to investigate the accuracy of parameter estimates as a function of full-width at half-maximum (*FWHM*) of IRF. The accuracy was characterized by E_{med} with corresponding SD. The results of simulations for two-exponential decays with equal amplitudes, one short lifetime $\tau_1 = 1.5h$, and no zero-time shift (Fig. 3) show that for QA and CA E_{med} does not differ significantly above $FWHM = 10h$ and both increase roughly linearly. The minima for these two approximations are achieved below $FWHM = 5h$, when both approximations sharply lose accuracy due to very coarse representation of the IRF. In contrast to performance of QA and CA, the linear approximation is not only always less accurate but achieves its minimum at relatively high value for *FWHM*, i.e., $\sim 16h$. Thus, Fig. 3 clearly demonstrates that there would be no point in narrowing the IRF, in our case to <150 ps, if LA is used. An IRF width of 150 ps is, in fact, much larger than IRF widths most often achieved with modern technology for time-correlated single-photon counting. Based on Fig. 3, the same argument can be mounted for QA and CA but, in this case, the optimal widths are at the limit of the most advanced technology currently available.

TABLE 7 The shortest lifetime recovery for three-component decays

PA	τ_1	$\bar{\tau}_1$	$CV(\tau_1)\%$	E_{med}	e_1^{max}	e_2^{max}	$\bar{e}$
			$\tau_2 = 100$, $\tau_3 = 1000$, $A_1{:}A_2{:}A_3 = 10{:}1{:}1$, $\delta = 0$, $\xi = 0.1$				
LA	13.0	10.2	12.0	0.153 (6)	0.405	0.069	$1.9 \cdot 10^{-3}$
QA	6.3	7.8	14.8	0.148 (12)	0.173	0.027	$1.9 \cdot 10^{-4}$
CA	6.2	7.4	13.6	0.121 (11)	0.122	0.017	$2.5 \cdot 10^{-5}$
			$\tau_2 = 750$, $\tau_3 = 1500$, $A_1{:}A_2{:}A_3 = 1{:}4{:}4$, $\delta = 8$, $\xi = 0.1$				
LA	140	173	14.4	0.085 (8)	0.459	0.366	$1.2 \cdot 10^{-2}$
QA	146	151	15.4	0.060 (5)	0.052	0.010	$2.6 \cdot 10^{-4}$
CA	146	151	15.4	0.061 (5)	0.032	0.009	$3.8 \cdot 10^{-5}$
				$\delta = -24$			
CA	160	173	14.3	0.068 (8)	0.026	0.022	$2.0 \cdot 10^{-4}$
			$\delta = 8$, $h = 5$, $n = 1024$, $C = 4 \cdot 10^4$				
LA	80	112	8.8	0.140 (3)	0.640	0.511	$1.5 \cdot 10^{-2}$
QA	55	59	12.7	0.044 (4)	0.077	0.057	$5.9 \cdot 10^{-4}$
CA	55	56	13.2	0.039 (4)	0.009	0.005	$2.8 \cdot 10^{-5}$

Notation as in Table 4. The values of lifetimes, zero-time shift, and channel width are expressed in picoseconds. If not otherwise stated, $h = 10$ ps, $n = 512$ channels, $FWHM = 100$ ps, $C = 2 \cdot 10^4$ counts.

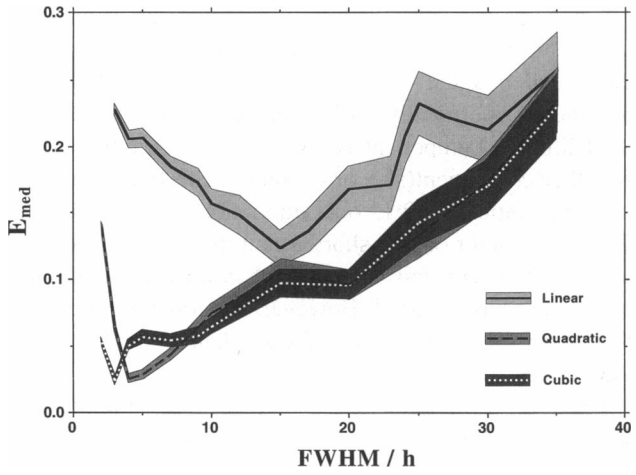

FIGURE 3 Accuracy of decay parameter estimation for the linear, quadratic, and cubic approximations as a function of full-width half-maximum of the instrument response function. The accuracy is represented by the median of the average relative error in parameters E_{med} (Eq. 39) and the respective SD illustrated by shaded areas. Fluorescence intensity decay curves were synthesized based on: $n = 512$ channels, $C = 2 \times 10^4$ counts, $h = 10$ ps, $\tau_1 = 15$ ps, $\tau_2 = 1000$ ps, $A_1 = A_2 = 0.5$, $\xi = 0.1$, $\delta = 0$, $b = 2$ counts.

Somewhat surprising results for the dependence of accuracy on the IRF width occur when there is a slight zero-time shift $\delta = 0.8h$ (Fig. 4). The performance of LA is then very good for very narrow IRF, but already at $FWHM = 10h$ the E_{med} becomes large and stays such as $FWHM$ increases. On the other hand, the increase in error for QA and CA is much more gradual and offers still relatively good accuracy for $FWHM = 30h$. The same level of accuracy is achieved by LA at 6 times narrower IRF. This is a clear demonstration of the advantage inherent in the use of higher order polynomial approximations.

Figs. 3 and 4 both show the variation in accuracy for QA and CA as $FWHM$ becomes of the order of few channel widths. The message of that observation is clear: narrowing the IRF really does improve accuracy, if at the same time we narrow the channel width so that $FWHM/h$ ratio is larger than 5.

In our final illustration, we consider a more complex three-component decay that actually was obtained in the time-resolved fluorescence study of human recombinant interferon α_2 (Vincent et al., 1992). The decay function (Fig. 2 *A* of Vincent et al., 1992) is characterized by a relatively short lifetime $\tau_1 = 160$ ps with a small amplitude $A_1 = 0.1$ (see the legend of Fig. 5 for other decay parameters). The channel width was $h = 15$ ps, and the IRF was roughly 3 times wider than τ_1, i.e., $FWHM = 500$ ps. We simulated this decay using $C = 6 \times 10^4$ which, according to Fig. 1 of Vincent et al. (1992), should correspond approximately to the actual measurement. Because no information on possible zero-time shift and scatter parameter was provided in this study, we assumed $\xi = 0.1$ and zero-time shift somewhat smaller than the channel width: $\delta = 13h/15$. The results of our simulations shown in Fig. 5 reveal pattern similar to that in Fig. 4. For $FWHM = 500$ ps, at which the actual measurements occurred, the advantage of applying either QA or CA is evident and it becomes more emphasized for decreasing width. Fig. 5 illustrates clearly that Vincent at al. would not have benefited in accuracy from narrowing the IRF while using the linear approximation unless they had narrowed the IRF to $FWHM$ below 100 ps). In contrast, by applying

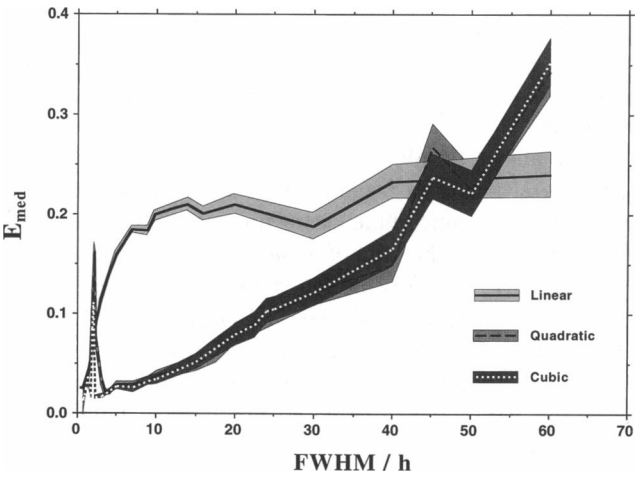

FIGURE 4 Accuracy of decay parameter estimation for the linear, quadratic, and cubic approximations as a function of full-width half-maximum of the instrument response function. The accuracy is represented by the median of the average relative error in parameters E_{med} (Eq. 39) and the respective SD illustrated by shaded areas. Fluorescence intensity decay curves were synthesized based on: $n = 512$ channels, $C = 2 \times 10^4$ counts, $h = 10$ ps, $\tau_1 = 30$ ps, $\tau_2 = 1000$ ps, $A_1 = A_2 = 0.5$, $\xi = 0.1$, $\delta = 8$ ps, $b = 2$ counts.

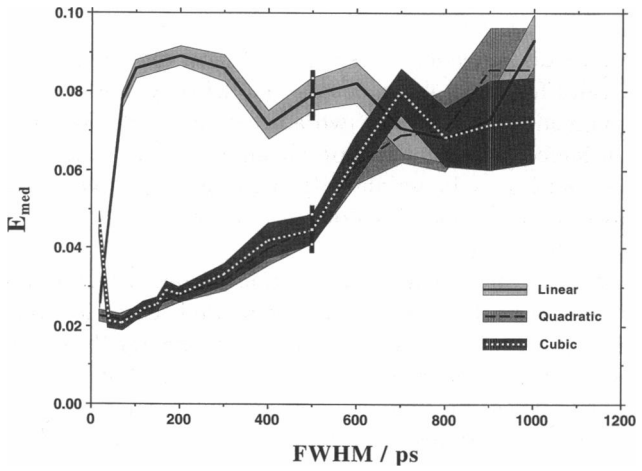

FIGURE 5 Accuracy of decay parameter estimation for the linear, quadratic, and cubic approximations as a function of full-width half-maximum of the instrument response function. The accuracy is represented by the median of the average relative error in parameters E_{med} (Eq. 39) and the respective SD illustrated by shaded areas. Fluorescence intensity decay curves were synthesized based on measurements of human recombinant interferon α_2: $\tau_1 = 160$ ps, $\tau_2 = 1640$ ps, $\tau_3 = 3840$ ps, $A_1 = 0.1$, $A_2 = 0.86$, $A_3 = 0.04$, $b = 6$ counts (for other parameters, see text).

CA or QA a continuous steady gain in accuracy is achieved by narrowing the IRF.

In a more idealistic case assuming no zero-time shift, the simulations based on data of Vincent et al. (1992) show that there is no significant difference in accuracy among LA, QA, and CA for $FWHM = 500$ ps: $E_{med}(LA) = 0.038 \pm 0.003$, $E_{med}(QA) = E_{med}(CA) = 0.033 \pm 0.002$. However, as the IRF becomes narrower, the difference becomes more emphasized (for example, at $FWHM = 100$ ps we obtained $E_{med}(LA) = 0.055 \pm 0.002$, $E_{med}(QA) = 0.020 \pm 0.001$, $E_{med}(CA) = 0.022 \pm 0.002$), and essentially the same pattern as in Fig. 5 is repeated. Thus, even in the most advantageous circumstances for LA, namely for $\delta = 0$, in this example one can benefit from use of the higher order polynomial approximations providing that a sufficiently narrow IRF is achieved.

CONCLUDING REMARKS

The principal achievement in this paper is the rigorous derivation of the general discretization formula for the fluorescence intensity deconvolution, which is valid not only for multiexponential decays but also for the nonexponential decays (e.g., Nemzek et al., 1974.; Van der Auweraar et al., 1982; Klafter and Schlesinger, 1986; Alcala, 1994). Although there is growing interest in modeling decays with functions different from multiexponential functions with limited number of components, we could find only a single reference to a simple piecewise constant approximation of convolution integral for such models (Argyrakis et al., 1991).

In our approach, the problem of discretizing the convolution integral is reduced to essentially one approximation step that includes approximation of the integrated IRF ("count function") over the range of only one channel. Wahl's discretization, which is used most often and which is valid for the multiexponential model only, involves approximation of IRF over two adjacent channels. We have considered polynomial approximations of the integrated IRF, but it may be worthwhile to consider approximations based on some other functions (e.g., of the form $at^b e^{ct} + d$) or fitting to cubic splines.

We have presented a discretization scheme, which is also more general than others in the literature because it explicitly allows for a zero-time shift. Computationally convenient expressions are provided for polynomial approximations to be used for the multiexponential decay model. For the linear, quadratic, and cubic approximations, we performed a large number of simulations that reveal that quadratic and cubic approximations yield more accurate recovery of parameters than does linear approximation. At the same time, there was no significant difference between quadratic and cubic approximations in terms of the accuracy achieved except when the zero-time shift becomes larger than the width of two channels. In that case, cubic approximation is best.

For the practitioner, the question now arises: What is the shortest lifetime one can recover from an heterogeneous decay under actual experimental circumstances? The answer depends critically on how large the amplitude of the short lifetime component is relative to the amplitude(s) of the other component(s). For example, if in two-component case this ratio is 10:1, our simulations show that even lifetimes a factor of five shorter than the channel width can be recovered with fair accuracy when quadratic and cubic approximations are used. However, for equal amplitudes at best lifetimes of the order of one channel width can be recovered.

The accuracy in model parameters recovery diminishes as the zero-time shift becomes larger in absolute value, but it is worth noting that moderate negative shifts influence the accuracy significantly less than positive shifts of equal magnitude. It is clear that the most desirable circumstances occur when the zero-time shift is negligible or can be avoided by use of a reference fluorophore. Večeř et al. (1993) has discussed approaches based on reference fluorophores in detail and proposed the so called REF reconvolution. It will be interesting to investigate how the present discretization scheme works for such types of deconvolution. We also need to determine the performance of the proposed scheme when a global analysis (Knutson et al., 1983; Beechem and Gratton, 1988) is used.

Using a number of simulations, we have essentially justified the common belief that a narrower IRF allows for better estimates of decay parameters. However, there is an optimum ratio of full-width at half-maximum of the IRF with respect to channel width, for which the estimates are most accurate. This ratio for quadratic and cubic approximations is ~5, whereas in some cases it is 15 when the linear approximation is applied. Our simulations thus support the idea that the effort to narrow the IRF may be in vain if linear approximation is used, even though such a tactic remains effective when quadratic or cubic approximations are applied.

In summary, for all of the reasons mentioned above, we recommend the use of quadratic or cubic approximations and do not recommend the use of linear approximation. We also recommend the use of simulations (based on some synthetic IRF, possibly obtained by simple least-squares fitting to data) whenever a suspiciously short lifetime is recovered and/or high χ^2_ν is obtained. Such simulations will reveal whether, under the experimental conditions used, the parameters recovered could have been determined accurately.

We are indebted to Mr. Miljenko Marušić for helpful advice regarding some mathematical aspects and to Mr. Miljenko Huzak and Mr. Joe Fitzpatrick for help in numerical work. We also thank Mr. Ken Peters for preparing the figures and Mr. Mahlon C. Stacy, who was extremely efficient in keeping our hardware running properly.

This work was supported by GM34847 of the PHS.

APPENDIX

The explicit expression for $K_{ij}(\delta)$ from Eq. 25 is

$$K_{ij}(\delta) = \bar{\theta}(t_{j-1} + \delta)I_{ij0}S_j + \sum_{\lambda=1}^{m} a[\theta(t_{j-1} + \delta)(J_{ijl} - I_{ijl} - J_{ij0}\delta^{\lambda}) + I_{ij\lambda}] \tag{40}$$

$$I_{ij\lambda} = \int_0^{t_{j+\delta}} (t - t_{j-1})^{\lambda} I(t_i - \delta - t)dt \tag{41}$$

$$J_{ij\lambda} = \int_0^{h} (t + \delta)^{\lambda} I(t_i - t_{j-1} - t)dt \tag{42}$$

The functions $\bar{\theta}(x)$ and $\theta(x)$ are defined by Eq. 24.

Next we present the explicit iterative formula for $\Delta_{ik}^{m}(\delta)$ from Eq. 30:

$$\Delta_{ik}^{m}(\delta) = A_k\tau_k \sum_{\lambda=0}^{m}\sum_{j=0}^{1}(-1)^j b_{i-j\lambda}\{\theta_{ji} \times [(1 - \theta_{ji-1})Y_{i-j\lambda} + \theta_{ji-1}X_{\lambda}] - \theta_{0i-1}f_{j\lambda}\} \tag{43}$$

$$\theta_{ji} = \theta(t_{i-j} + \delta), \qquad b_{i\lambda} = h^{\lambda}a_{i\lambda}, \qquad b_{0\lambda} = 0, \tag{44}$$

$$b_{i0} = (1 - \delta_{i1})\sum_{\nu=1}^{i-1} R_{\nu}, \qquad i = 1, \ldots, n,$$

$$f_{j\lambda} = (1 - D_k)(j + d)^{\lambda}, \qquad d = \delta/h, \qquad D_k = e^{-p_k}, \qquad p_k = h/\tau_k, \tag{45}$$

$$Y_{i\lambda} = (1 + d)^{\lambda} - (1 - i)^{\lambda}D_k^{i+d} - \lambda p_k^{-1}Y_{i\lambda-1}, \qquad Y_{i0} = 1 - D_k^{i+d}, \tag{46}$$

$$X_{\lambda} = (1 + d)^{\lambda} - d^{\lambda}D_k - \lambda p_k^{-1}X_{\lambda-1}, \qquad X_0 = 1 - D_k. \tag{47}$$

The equations are defined for $i \geq 0$, $\lambda = 1, \ldots, m$. This expression for $\Delta_{ik}^{m}(\delta)$ can be implemented easily in a computer program.

REFERENCES

Alcala, J. R. 1994. The effect of harmonic conformational trajectories on protein fluorescence and lifetime distributions. *J. Chem. Phys.* 101: 4578–4584.

Argyrakis, P., G. Duportail, P. Lianos. 1991. Behaviour of the rate constant for reactions in restricted spaces: fluorescence probing of lipid vesicles. *J. Chem. Phys.* 95:3808–3814.

Bajzer, Ž., J. C. Sharp, S. S. Sedarous, and F. G. Prendergast. 1990. Padé-Laplace method for the analysis of time resolved fluorescence decay curves. *Eur. Biophys. J.* 18:101–115.

Bajzer, Ž., T. M. Therneau, J. C. Sharp, and F. G. Prendergast. 1991. Maximum likelihood method for the analysis of time-resolved fluorescence decay curves. *Eur. Biophys. J.* 20:247–262.

Bajzer, Ž., and F. G. Prendergast. 1992. Maximum likelihood analysis of fluorescence data. *Methods Enzymol.* 210:200–237.

Beechem, J. M., and E. Gratton. 1988. Fluorescence spectroscopy data analysis environment: a second generation Global analysis program. *SPIE Proc.* 909:70–81.

Eisenfeld, J., and C. C. Ford. 1979. A systems theory approach to the analysis of multiexponential fluorescence decay. *Biophys. J.* 26:73–84.

Grinvald, A., and I. Z. Steinberg. 1974. On the analysis of fluorescence decay kinetics by the method of least squares. *Anal. Biochem.* 59: 583–598.

Holtom, G. R. 1990. Artifacts and diagnostics in fast fluorescence measurements. *SPIE Proc.* 1204:2–12.

Klafter, J., and M. F. Shlesinger. 1986. On the relationship among three theories of relaxation in distorted systems. *Proc. Natl. Acad. Sci. USA.* 83:848–851.

Knutson, J. R., J. M. Beechem, and L. Brand. 1983. Simultaneous analysis of multiple fluorescence decay curves: a global approach. *Chem. Phys. Lett.* 102:501–507.

Livesey, A. K., and J. C. Brochon. 1987. Analyzing the distribution of decay constants in pulse-fluorometry using the maximum entropy method. *Biophys. J.* 52:693–706.

McKinnon, A. E., A. G. Szabo, and D. R. Miller. 1977. The deconvolution of photoluminescence data. *J. Phys. Chem.* 81:1564–1567.

More, J. J. 1977. The Levenberg-Marquardt algorithm: implementation and theory. *In* Numerical Analysis. G. A. Watson, editor. Springer Verlag, New York.

Morris, A. H., Jr. 1981. NSWC/DL Library of Mathematical Subroutines. Naval Surface Weapons Centre, Dahlgren, VA.

Nemzek, T. L., and W. R. Ware. 1974. Kinetics of diffusion-controlled reactions: transient effects in fluorescence quenching. *J. Chem. Phys.* 62:477–490.

O'Connor, D. V., and D. Phillips. 1984. Time-Correlated Single Photon Counting. Academic Press, New York.

Periasamy, N. 1988. Analysis of fluorescence decay by the nonlinear least-squares method. *Biophys. J.* 54:961–967.

Press, W. H., B. P. Flannery, S.A. Teukolsky, and W. T. Vetterling. 1986. Numerical Recepies. Cambridge University Press, Cambridge. 289 pp.

Rade, L., and B. Westergren. 1990. Beta Mathematics Handbook. CRC Press, Boca Raton, FL.

Van der Auweraer, M., C. Dederen, C. Palmans-Windels, and F. C. De Schryver. 1982. Fluorescence quenching by neutral molecules in sodium dodecyl sulfate micelles. *J. Am. Chem. Soc.* 104:1800–1804.

Večer, J., A. A. Kowalczyk, and R. E. Dale. 1993. Improved recursive convolution integral for the analysis of fluorescence decay data: local approximation of the apparatus response. *Rev. Sci. Instr.* 64:3403–3412.

Vincent, M., I. M. Li De La Sierra, M. N. Berberan-Santos, A. Diaz, M. Diaz, G. Padron, and J. Gallay. 1992. Time-resolved fluorescence study of human recombinant interferon α_2. *Eur. J. Biochem.* 210:953–961.

Wahl, Ph. 1979. Analysis of fluorescence anisotropy decays by a least square method. *Biophys. Chem.* 10:91–104.

Ware, W. R., L. J. Doemeny, and T. L. Nemzek. 1973. Deconvolution of fluorescence and phosphorescence decay curves: a least-squares method. *J. Phys. Chem.* 77:2038–2048.